Oxygen ion conductivity of $La_{0.8}Sr_{0.2}Ga_{0.83}Mg_{0.17-x}Co_xO_{3-\delta}$ synthesized by laser rapid solidification*

Zhang Jie(张 洁)[a)b)], Yuan Chao(袁 超)[c)], Wang Jun-Qiao(王俊俏)[a)], Liang Er-Jun(梁二军)[a)†], and Chao Ming-Ju(晁明举)[a)]

[a)] School of Physical Science & Engineering and Key Laboratory of Materials Physics of Ministry of Education of China, Zhengzhou University, Zhengzhou 450052, China

[b)] Department of Physics and Electronic Science, Zhengzhou Normal University, Zhengzhou 450044, China

[c)] College of Science, Henan Agricultural University, Zhengzhou 450002, China

(Received 1 November 2012; revised manuscript received 15 January 2013)

Materials $La_{0.8}Sr_{0.2}Ga_{0.83}Mg_{0.17-x}Co_xO_{3-\delta}$ with $x = 0$, 0.05, 0.085, 0.10, and 0.15 are synthesized by laser rapid solidification. It is shown that the samples prepared by laser rapid solidification give rise to unique spear-like or leaf-like microstructures which are orderly arranged and densely packed. Their electrical properties each show a general dependence of the Co content and the total conductivities of $La_{0.8}Sr_{0.2}Ga_{0.83}Mg_{0.085}Co_{0.085}O_{3-\delta}$ prepared by laser rapid solidification are measured to be 0.067, 0.124, and 0.202 S·cm^{-1} at 600, 700, and 800 °C, respectively, which are much higher than by conventional solid state reactions. Moreover, the electrical conductivities each as a function of the oxygen partial pressure are also measured. It is shown that the samples with the Co content values ≤ 8.5 mol% each exhibit basically ionic conduction while those for Co content values ≥ 10 mol % each show ionic mixed electronic conduction under oxygen partial pressures from 10^{-16} atm (1 atm = 1.01325×10^5 Pa) to 0.98 atm. The improved ionic conductivity of $La_{0.8}Sr_{0.2}Ga_{0.83}Mg_{0.085}Co_{0.085}O_{3-\delta}$ prepared by laser rapid solidification compared with by solid state reactions is attributed to the unique microstructure of the sample generated during laser rapid solidification.

Keywords: doped lanthanum gallate, laser rapid solidification, oxygen ion conductivity, activation energy

PACS: 72.60.+g, 61.72.U–, 66.90.+r **DOI:** 10.1088/1674-1056/22/8/087201

1. Introduction

Solid oxide fuel cells (SOFCs) have attracted great attention because of their high energy conversion efficiencies, little pollution, and widely flexible fuel choices. Yttria-stabilized zirconia (YSZ) is the most commonly used electrolyte in SOFCs, which requires operating temperature around 1000 °C. However, the high temperature leads to a series of complicated material problems, such as high-temperature gas seal, mismatch in thermal expansion coefficients between different parts, interface reactions, etc. Therefore, a major challenge in reducing the operating temperature of SOFCs is to develop alternative electrolyte materials that can operate at intermediate-temperatures (500 °C–800 °C) with high oxygen-ion conductivity.[1,2] Among those conductors,[3–6] Sr^{2+}- and Mg^{2+}-doped $LaGaO_3$, $La_{1-x}Sr_xGa_{1-y}Mg_yO_{3-\delta}$ (LSGM), were each shown to have a high oxide-ion conductivity in a temperature range of 600 °C–800 °C which is about four times larger than that of the conventional YSZ solid electrolyte at 700 °C.[7,8] Among the perovskite structures of $La_{1-x}Sr_xGa_{1-y}Mg_yO_{3-\delta}$, the composition of $La_{0.8}Sr_{0.2}Ga_{0.83}Mg_{0.17}O_{2.815}$ seems to be the most promising one for SOFCs since it gives rise to the best ionic conductivity in the LSGMs.[8]

The electrical properties of LSGM can also be modified by partial substitution of the Ga site by transition metals (Cr, Mn, Fe, Co, and Ni).[9–19] The reported results showed that Ni, Mn, and Cr doping enhanced the electron and hole conduction while Fe or Co doped-LSGMs gave rise to higher oxide-ion conductivity.[9–11,17,18] Among all transition metal cations examined, cobalt was found to be the most effective dopant for increasing the oxide-ion conductivity.[9,10,12,13] Ishihara *et al.*[10] found the optimum composition for ionic conductivity to be $La_{0.8}Sr_{0.2}Ga_{0.8}Mg_{0.115}Co_{0.085}O_{3-\delta}$, considering the transport number and ion transport number.[10] Following these reports, numerous experimental studies have been carried out on the Co-doped $La_{0.8}Sr_{0.2}Ga_{0.8}Mg_{0.2}O_{2.8}$[20–23] and $La_{0.9}Sr_{0.1}Ga_{0.8}Mg_{0.2}O_{2.85}$.[24]

Though $La_{0.8}Sr_{0.2}Ga_{0.83}Mg_{0.17}O_{2.815}$ has the best ionic conductivity in $La_{1-x}Sr_xGa_{1-y}Mg_yO_{3-\delta}$ systems, to our knowledge, the systemic study on the effect of Co-doping on this composition has not been reported so far. In a previous study, laser rapid solidification (LRS) was used to synthesize $La_{0.9}Sr_{0.1}Ga_{0.8}Mg_{0.2}O_{2.85}$ electrolyte.[25] It showed that the LSGM prepared by LRS exhibited unique microstructure and superior electrical properties compared with by solid state reactions (SSR). In this paper, we report on the syntheses of $La_{0.8}Sr_{0.2}Ga_{0.83}Mg_{0.17-x}Co_xO_{3-\delta}$ ($x = 0$, 0.05, 0.085, 0.10,

*Project supported by the National Natural Science Foundation of China (Grant No. 10974183), the Fund for Science and Technology Innovation Team of Zhengzhou City, China (Grant No. 2011-3), and the Postdoctoral Research Sponsorship in Henan Province, China (Grant No. 2011002).

†Corresponding author. E-mail: ejliang@zzu.edu.cn

© 2013 Chinese Physical Society and IOP Publishing Ltd

0.15) prepared by LRS and study the effect of Co doping on the electrical properties of $La_{0.8}Sr_{0.2}Ga_{0.83}Mg_{0.17}O_{2.815}$. In fact, whether the LRS technique can be used to synthesize Co-doped $La_{0.8}Sr_{0.2}Ga_{0.83}Mg_{0.17}O_{2.815}$ also needs to be tested, for it succeeds in the syntheses of ZrW_2O_8, HfW_2O_8, $Y_2Mo_3O_{12}$, and so on. but fails in the syntheses of $ZrMo_2O_8$ and $HfMo_2O_8$.[26–28] It is shown that not only the LRS technique can be used for synthesizing $La_{0.8}Sr_{0.2}Ga_{0.83}Mg_{0.17-x}Co_xO_{3-\delta}$, but also the LRS can prepare the samples that exhibit very unique microstructure and very high electrical conductivity compared with the Co-doped LSGMs prepared by SSR. Particularly, the $La_{0.8}Sr_{0.2}Ga_{0.83}Mg_{0.085}Co_{0.085}O_{3-\delta}$ synthesized by LRS gives rise to significantly higher ionic conductivity than by SSR in an oxygen partial pressure ($p(O_2)$) range from 10^{-16} atm (1 atm = 1.01325×10^5 Pa) to 0.98 atm at 800 °C.

2. Experiment

La_2O_3 (99.99%), Ga_2O_3 (99.99%), MgO (99.99%), $SrCO_3$ (99%), and Co_2O_3 (99.9%) were used as the starting materials. La_2O_3 and MgO were fired at 1000 °C for 7 h before weighting to decompose carbonate and hydroxide impurities. The absence of impurities in the reagents was checked by X-ray diffraction (XRD). The starting materials were mixed with stoichiometric ratios of the destination materials of $La_{0.8}Sr_{0.2}Ga_{0.83}Mg_{0.17-x}Co_xO_{3-\delta}$ ($x = 0$, 0.05, 0.085, 0.10, 0.15), ground in a mortar for 2 h and then pressed into cuboid bars (40 mm × 5 mm × 5 mm) or disks of 15 mm in diameter and 3.0 mm in thickness by uni-axial cold press with a steel mould at a pressure of 10 MPa and dried for 2 h at 100 °C in a baking oven before sintering. The synthesis of the samples was performed by using a 5-kW continuous-wave CO_2 laser. Figure 1 shows the schematic diagram of the experimental set-up of LRS, mainly including a CO_2 laser, a device controlling power, a sample platform which can move horizontally and a laser power meter recording the laser power during the LRS process. The laser beam impinged onto a bar placed at a distance where the defocus length was set to be 120 mm. The beam spot on the sample was approximately 12 mm in diameter. The optimized synthesis conditions were 1100-W laser power and 1-mm·s^{-1} scan speed. As the laser beam moved ahead along the length direction, the synthesized sample behind cooled naturally and rapidly down to room temperature. For comparison, samples of $La_{0.8}Sr_{0.2}Ga_{0.83}Mg_{0.085}Co_{0.085}O_{3-\delta}$ were also prepared by SSR through calcinating the disks at 1250 °C for 10 h and then sintering at 1500 °C for 6 h and finally sintering at 1600 °C for 2 h with intermediate grindings. Compared with the solid state reactions, the LRS is a rapid process, with which a sample can be synthesized within tens of seconds. The densities of the sintered samples were measured via the Archimedes method.

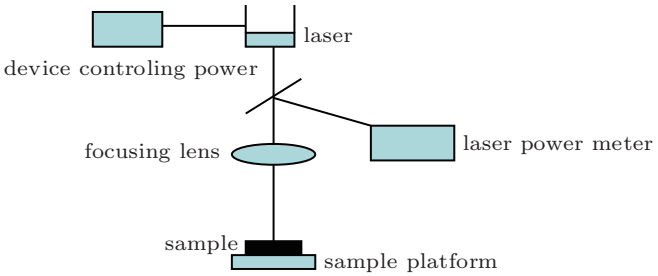


Fig. 1. (color online) Schematic diagram of the experimental set-up of LRS.

The samples were analyzed by XRD with an X'Pert PRO X-ray diffractometer. The microstructures were studied with a JSM-6700F scanning electron microscope (SEM). The laser sintered bars were re-melted by laser and polished into cylinders or cuboids with dimensions Φ8.50 mm × 3.40 mm ($x = 0.0$), Φ13.72 mm × 4.20 mm ($x = 0.05$), 10.00 mm × 6.97 mm × 3.94 mm ($x = 0.085$), Φ10.50 mm × 2.72 mm ($x = 0.10$), and Φ10.40 mm × 3.26 mm ($x = 0.15$), and the sample prepared by solid state reactions was polished into a size of 6.40 mm×5.52 mm×2.50 mm for electrical measurements. Platinum paste was used to smear both faces of the cuboids or pellets, and Pt wires were connected to a Pt mesh followed by calcination at 950 °C for 30 min. The conductivity of each sample was measured in air as a function of temperature (250 °C–800 °C) by AC impedance spectra with Parstat 2273 (Princeton Applied Research). The range of AC frequency was 0.1 Hz–10^6 Hz. The impedance spectra were fitted using ZSimpWin 3.0 software to obtain the resistances. The electrical properties in this paper are given for samples of 1 cm^2 × 1 cm. The electrical conductivities each as a function of oxygen partial pressure were measured by impedance method using electrochemical workstations (Zahner IM6ex) in a gas flow system. The partial pressure of oxygen was controlled by mixing Ar or H_2 with O_2, and the oxygen partial pressure was monitored by an oxygen sensor made of Y_2O_3-stabilized ZrO_2 that was attached close to the sample.

3. Results and discussion

3.1. Phase composition

Figure 2 shows the XRD patterns of $La_{0.8}Sr_{0.2}Ga_{0.83}Mg_{0.17-x}Co_xO_{3-\delta}$ synthesized by LRS for $x = 0$, 0.05, 0.085, 0.10, 0.15 and by SSR for $x = 0.085$, respectively. It shows that the $La_{0.8}Sr_{0.2}Ga_{0.83}Mg_{0.17-x}Co_xO_{3-\delta}$ perovskites can be successfully synthesized by LRS except the one with $x = 0.15$ which contains a few secondary phases of $LaSrGa_3O_7$. With Co content increasing, the diffraction peaks at higher angles split, indicating the lowering of the crystal symmetry. Besides, the diffraction peaks shift toward higher angles with Co content increasing, suggesting that the lattice

constants become smaller by Co doping and a solid solution of Co doped at the Ga site in the lattice is realized,[10] for the ionic size of the six-coordinated Co^{3+} (63 pm) is smaller than that of Mg^{2+} (66 pm) and nearly the same as that of the six-coordinated Ga^{3+} ion (62 pm).[10] As an example, figure 3 shows Rietveld analysis of the XRD pattern of $La_{0.8}Sr_{0.2}Ga_{0.83}Mg_{0.17}O_{2.815}$ for *Imma* at room temperature with Bragg R factor = 6.2% and $R_{wp}/R_e = 1.79$. It can be seen that $La_{0.8}Sr_{0.2}Ga_{0.83}Mg_{0.17}O_{2.815}$ can be fitted to an orthorhombic structure (*Imma*) with acceptable values for Bragg R factor and R_{wp}/R_e. In this way the lattice parameters of all $La_{0.8}Sr_{0.2}Ga_{0.83}Mg_{0.17-x}Co_xO_{3-\delta}$ samples are estimated on the same basis of an orthorhombic lattice taken from that of $La_{0.9}Sr_{0.1}Ga_{0.8}Mg_{0.2}O_{2.85}$ by Rietveld refinement. Figure 4 shows the lattice parameters (a, b, and c) of the specimens prepared by LRS each as a function of Co content. Due to the substitution of Mg^{2+} by six-coordinated Co^{3+}, the lattice parameters a, b, and c basically decrease with Co content increasing.

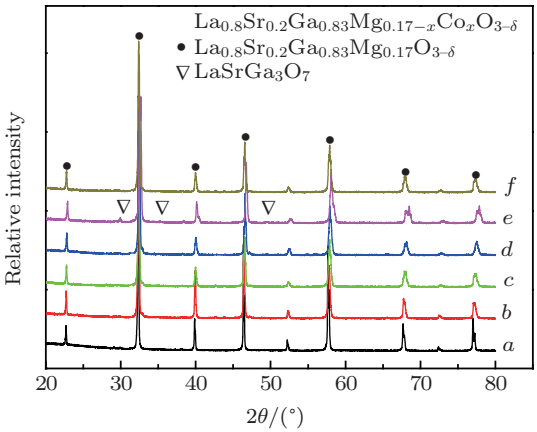


Fig. 2. (color online) XRD patterns of $La_{0.8}Sr_{0.2}Ga_{0.83}Mg_{0.17-x}Co_xO_{3-\delta}$ for $x = 0$ (curve a), 0.05 (curve b), 0.085 (curve c), 0.10 (curve d), and 0.15 (curve e), synthesized by LRS with 1100-W laser power at 1 mm·s^{-1} scan speed, and $x = 0.085$ (curve f), synthesized by SSR (1250 °C for 10 h, 1500 °C for 6 h, and 1600 °C for 2 h).

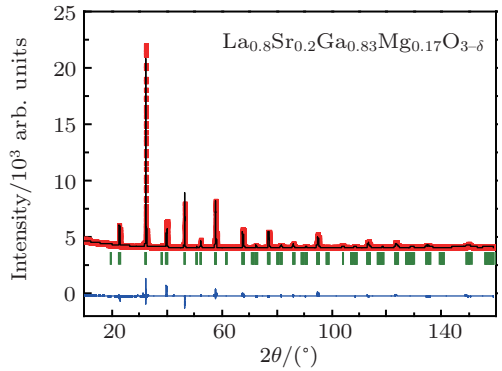


Fig. 3. (color online) Rietveld analyses of the XRD pattern of $La_{0.8}Sr_{0.2}Ga_{0.83}Mg_{0.17}O_{2.815}$ for *Imma* at room temperature with Bragg R factor = 6.2% and $R_{wp}/R_e = 1.79$. The bars (middle) indicate the positions of Bragg peaks for $La_{0.8}Sr_{0.2}Ga_{0.83}Mg_{0.17}O_{2.815}$. The dotted and solid lines (top) and the solid line (bottom) are the observed and calculated XRD patterns and difference profile, respectively.

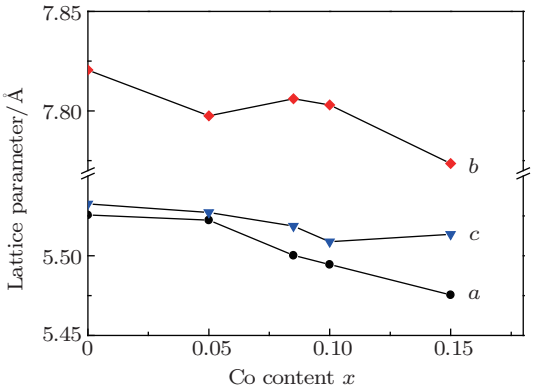


Fig. 4. (color online) Lattice parameters (a, b, and c) of $La_{0.8}Sr_{0.2}Ga_{0.83}Mg_{0.17-x}Co_xO_{3-\delta}$ each as a function of Co content for the samples prepared by LRS with 1100-W laser power at 1 mm·s^{-1} scan speed.

3.2. Unique microstructure

Figure 5 shows the typical SEM images of the fractured cross sections of $La_{0.8}Sr_{0.2}Ga_{0.83}Mg_{0.17-x}Co_xO_{3-\delta}$ prepared by LRS for $x = 0$, 0.05, 0.085, 0.10, 0.15 and by SSR for $x = 0.085$, respectively. While the sample of $La_{0.8}Sr_{0.2}Ga_{0.83}Mg_{0.085}Co_{0.085}O_{3-\delta}$ synthesized by SSR consists of densely packed globose grains that are similar to the reported LSGMs and Co-doped LSGMs in microstructure,[20,21,24] and the samples prepared by LRS give rise to unique microstructures exhibiting ordered or oriented spear-like (Figs. 5(a) and 5(c)) or leaf-like (Figs. 5(b), 5(d), and 5(e)) crystalline growth. The unique microstructures have not been observed previously for LSGMs and Co-doped LSGMs. The average grain sizes of the samples prepared by LRS are about 20 μm–50 μm (Figs. 5(a), 5(b), 5(d), and 5(e)) or larger than 50 μm (Fig. 5(c)) in width and longer than 50 μm in length. The relative densities of the samples prepared by LRS for $x = 0$, 0.05, 0.085, 0.10, 0.15 and by SSR for $x = 0.085$ were measured to be 97.2%, 96.1%, 98.7%, 98.5%, 98.1%, and 97.1%, respectively.

The laser synthetic route is a rather rapid process, during which the raw materials are heated to melt immediately upon illumination of the laser beam and form a molten pool where the chemical reaction takes place. The product solidifies rapidly as the laser beam moves ahead. The whole process from the laser starting to irradiate to the solidification of the final product is completed in only a few or tens of seconds. Both the XRD and the SEM images demonstrate that the starting materials were sufficiently molten in the molten pool. Otherwise, it is difficult to imagine for the raw materials to react completely to reach pure final products with nicely ordered microstructures in such a short time. Since the melting points of the raw materials of La_2O_3, $SrCO_3$, Ga_2O_3, and MgO are about 2315, 1497, 1740, and 2827 °C, respectively, the temperature of the molten pool is expected to be above 2830 °C. Another special characteristic of the LRS is the directed heat

transfer. The heat transfer was mainly directed from the top surface to the bottom and also governed by the moving direction of the laser beam as the laser energy was absorbed by the top layer of the raw materials. The unique microstructures of the samples are likely to result from convection in the molten LSGM specimens. The unique microstructures of the samples produced in the laser synthetic route can be attributed to the relatively oriented crystalline growth governed by heat transfer directions in the liquid droplet-like molten pool. Due to the rapid solidification from the molten pool, highly densely-packed blocks of the samples can be easily achieved.

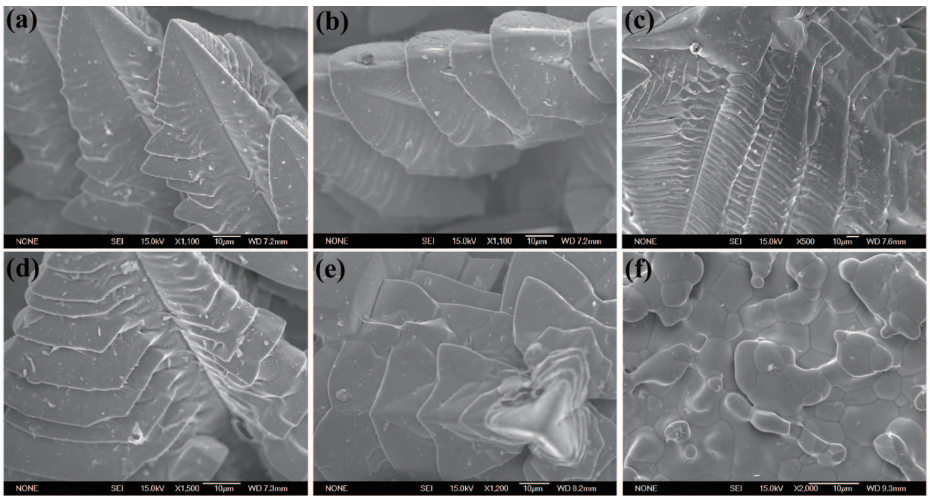


Fig. 5. (color online) SEM images of the fractured cross sections of $La_{0.8}Sr_{0.2}Ga_{0.83}Mg_{0.17-x}Co_xO_{3-\delta}$ for $x = 0$ (a), 0.05 (b), 0.085 (c), 0.10 (d), and 0.15 (e), synthesized by LRS with 1100-W laser power at 1 mm·s^{-1} scan speed, and $x = 0.085$ (f), synthesized by SSR (1250 °C for 10 h, 1500 °C for 6 h, and 1600 °C for 2 h).

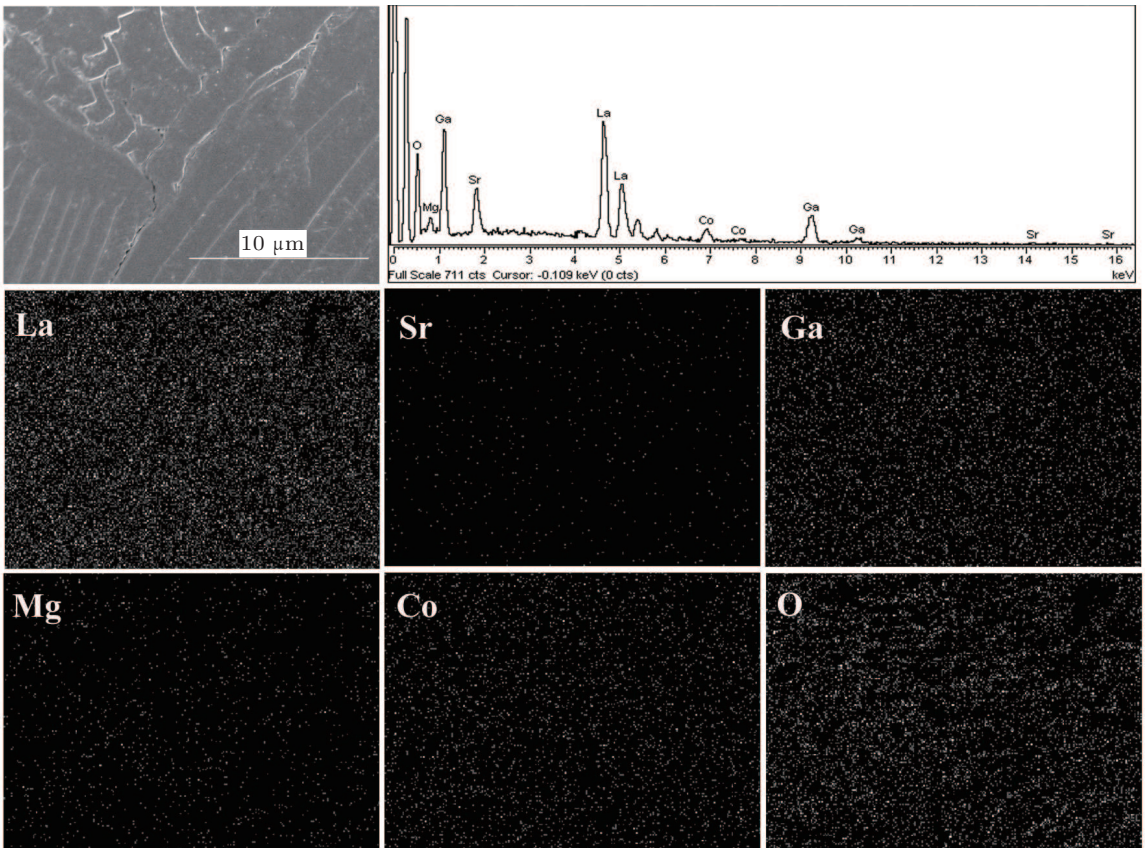


Fig. 6. Elemental mapping and EDS spectrum of $La_{0.8}Sr_{0.2}Ga_{0.83}Mg_{0.085}Co_{0.085}O_{3-\delta}$ synthesized by LRS.

Figure 6 shows the elemental mapping and the EDS spectrum for the sample of $La_{0.8}Sr_{0.2}Ga_{0.83}Mg_{0.085}Co_{0.085}O_{3-\delta}$ synthesized by laser rapid solidification. It is evident that the La, Sr, Ga, Mg, Co, and O are homogeneously dispersed in the sample of $La_{0.8}Sr_{0.2}Ga_{0.83}Mg_{0.085}Co_{0.085}O_{3-\delta}$. The approximate content values of elements for the sample of $La_{0.8}Sr_{0.2}Ga_{0.83}Mg_{0.085}Co_{0.085}O_{3-\delta}$ are given as listed in the Table 1. The atomic ratio of the La:Sr:Ga:Mg:Co:O in the pure $La_{0.8}Sr_{0.2}Ga_{0.83}Mg_{0.085}Co_{0.085}O_{3-\delta}$ prepared by laser rapid solidification is close to its nominal stoichiometric proportion 8.00:2.00:8.30:0.85:0.85:28.15. Figure 7 shows the X-ray photoelectron spectrum (XPS) (Co 2p) of $La_{0.8}Sr_{0.2}Ga_{0.83}Mg_{0.085}Co_{0.085}O_{3-\delta}$ to reveal the valence state of Co. The prominent peak around 779.7 eV is attributed to a Co^{3+} $2p_{3/2}$ configuration while the shoulder around 783.4 eV is ascribed to a Co^{2+} $2p_{3/2}$ configuration. The other spin–orbit components of the $2p_{1/2}$ appear at 791.3 eV and 796.4 eV for $Co^{3+}$and Co^{2+}, respectively. The peak at 802.9 eV is Co^{2+}shake-up satellite peak of the sample. It can be concluded that both Co^{3+} and Co^{2+} exist in $La_{0.8}Sr_{0.2}Ga_{0.83}Mg_{0.085}Co_{0.085}O_{3-\delta}$ but Co^{3+} is dominant in the sample.

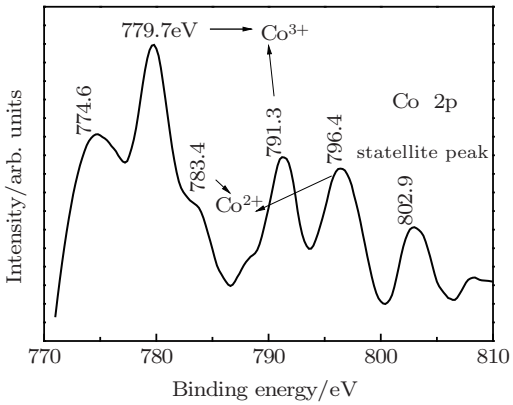


Fig. 7. XPS (Co 2p) of $La_{0.8}Sr_{0.2}Ga_{0.83}Mg_{0.085}Co_{0.085}O_{3-\delta}$ prepared by LRS with 1100-W laser power at 1 mm·s^{-1} scan speed.

Table 1. Atomic percents of the sample of $La_{0.8}Sr_{0.2}Ga_{0.83}Mg_{0.085}Co_{0.085}O_{3-\delta}$ synthesized by LRS from EDS measurements.

Element	Atomic %
La	16.62
Sr	4.24
Ga	17.13
Mg	1.72
Co	2.05
O	58.24

3.3. Electrical properties

We have measured the impedance spectra from 250 °C to 800 °C in steps of 50 °C for all the samples. Figure 8 shows a typical impedance spectrum of the sample $La_{0.8}Sr_{0.2}Ga_{0.83}Mg_{0.17}O_{2.815}$ at 250 °C. The higher, medium, and lower frequency arcs represent the bulk (R_b), grain boundary (R_{gb}), and electrode (R_e) responses, respectively.[29–31] The total resistance of the sample, obtained from the intercept of the spectra with the real-axis at high frequencies, which is indicated by the first vertical line in Fig. 8, is thus the sum of R_b and R_{gb}.

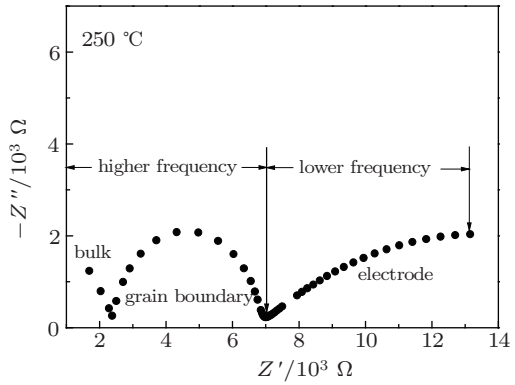


Fig. 8. The representative AC impedance spectrum of $La_{0.8}Sr_{0.2}Ga_{0.83}Mg_{0.17}O_{2.815}$ at 250 °C prepared by LRS with 1100-W laser power at 1 mm·s^{-1} scan speed.

Figure 9 shows the experimental and calculated impedance spectra of $La_{0.8}Sr_{0.2}Ga_{0.83}Mg_{0.17-x}Co_xO_{3-\delta}$ at 700 °C for $x = 0$, 0.05, 0.085, 0.10, and 0.15 prepared by LRS and for $x = 0.085$ prepared by SSR, respectively. It is evident that the total resistances of $La_{0.8}Sr_{0.2}Ga_{0.83}Mg_{0.17-x}Co_xO_{3-\delta}$ prepared by LRS each show a general decrease with Co content increasing except that for $x = 0.15$ and the lowest total resistances exist in the samples for $x = 0.085$–0.10. The higher resistance for $x = 0.15$ may result from the impurities found in Fig. 2. The $La_{0.8}Sr_{0.2}Ga_{0.83}Mg_{0.085}Co_{0.085}O_{3-\delta}$ prepared by LRS gives rise to a much lower total resistance than by SSR.

The total conductivities are calculated by fitting the experimental data according to equivalent circuits comprised of resistance R, capacitance C, and CPE (constant phase element) in series and/or in parallel.[25] The electrolyte resistance R, sum of grain resistance R_b, and grain boundary resistance R_{gb}, can be calculated by fitting the impedance spectra using ZSimpWin 3.0 software. The conductivity σ can then be calculated from

$$\sigma = \frac{L}{RA}, \tag{1}$$

where L is the thickness, and A the area of the cross section of an electrolyte sample.

The calculated total conductivities of the samples in a temperature range from 250 °C to 800 °C are calculated and shown in Table 2. It is obvious that the total conductivities are obviously improved by Co doping, showing a general increase with Co content increasing except that for $x = 0.15$. The total conductivities of $La_{0.8}Sr_{0.2}Ga_{0.83}Mg_{0.085}Co_{0.085}O_{3-\delta}$ prepared by LRS reach 0.067, 0.124, and 0.202 S·cm^{-1} at 600, 700, and 800 °C, respectively, which are much higher than the corresponding values (0.026, 0.065, and 0.105 S·cm^{-1}) of the same compositions with similar values of purity and relative density, prepared by SSR. The higher total conductivities

of the samples synthesized by LRS may be attributed to their unique microstructures. The relatively oriented growth of the spear-like or leaf-like grains with large and regular sizes and higher relative densities greatly reduces the scattering probabilities of charge carriers during migration, thereby increasing the conductivities.

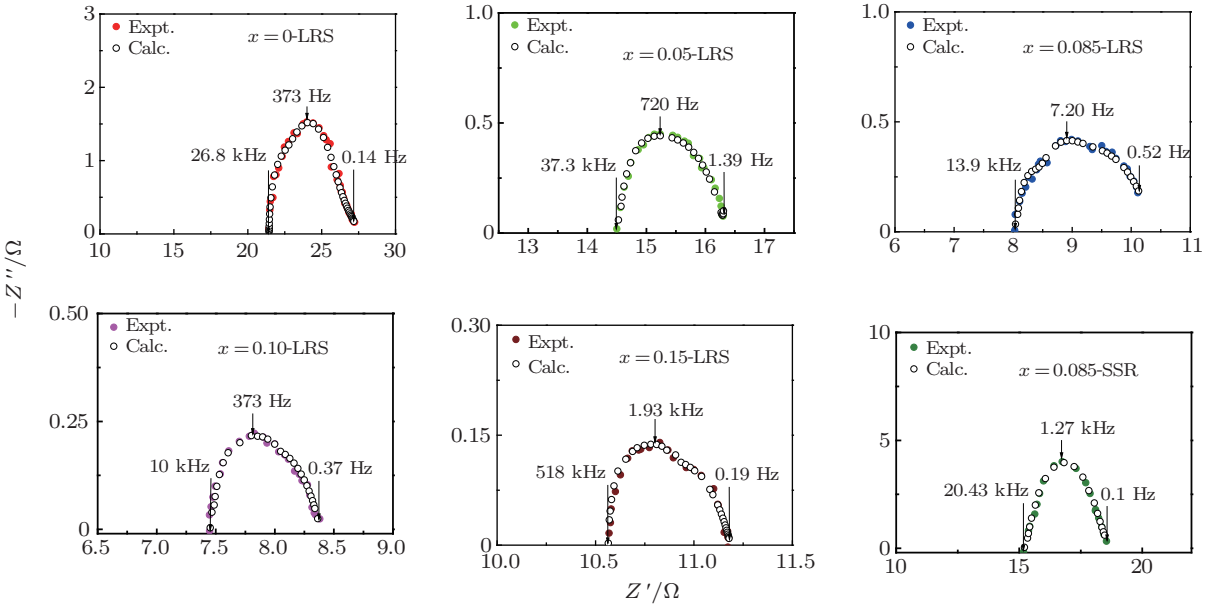


Fig. 9. (color online) AC impedance spectra measured at 700 °C in air for $La_{0.8}Sr_{0.2}Ga_{0.83}Mg_{0.17-x}Co_xO_{3-\delta}$ with $x = 0.0$, 0.05, 0.085, 0.10, and 0.15, prepared by LRS with 1100-W laser power at 1 mm·s^{-1} scan speed and with $x = 0.085$, prepared by SSR (sintered at 1250 °C for 10 h, 1500 °C for 6 h, and 1600 °C for 2 h).

Table 2. Electrical properties of $La_{0.8}Sr_{0.2}Ga_{0.83}Mg_{0.17-x}Co_xO_{3-\delta}$ for $x = 0.0$, 0.05, 0.085, 0.10, and 0.15 prepared by LRS and for $x = 0.085$ prepared by SSR.

Co content x		Total conductivity/S·cm^{-1}			Activation energy/eV		
		600 °C	700 °C	800 °C	250 °C–450 °C	450 °C–600 °C	600 °C–800 °C
LRS	$x = 0$	0.018	0.047	0.090	0.64	0.69	0.74
	$x = 0.05$	0.032	0.069	0.114	0.53	0.56	0.59
	$x = 0.085$	0.067	0.124	0.202	0.37	0.39	0.53
	$x = 0.10$	0.091	0.134	0.165	0.25	0.30	0.32
	$x = 0.15$	0.073	0.095	0.122	0.28	0.28	0.29
SSR	$x = 0.085$	0.026	0.065	0.105	0.72	0.67	0.64

Figure 10 shows the Arrhenius plots of the total conductivities of $La_{0.8}Sr_{0.2}Ga_{0.83}Mg_{0.17-x}Co_xO_{3-\delta}$ for $x = 0.0$, 0.05, 0.085, 0.10, and 0.15 prepared by LRS and for $x = 0.085$ prepared by SSR, respectively. It is seen that the slopes of the Arrhenius plots of the samples prepared by LRS decrease with Co content increasing, suggesting that the activation energy for electrical conduction decreases when the Co content is increased. Besides, the activation energy of $La_{0.8}Sr_{0.2}Ga_{0.83}Mg_{0.085}Co_{0.085}O_{3-\delta}$ synthesized by LRS is lower than by SSR. In Table 2, we summarize the activation energies of $La_{0.8}Sr_{0.2}Ga_{0.83}Mg_{0.17-x}Co_xO_{3-\delta}$ for $x = 0.0$, 0.05, 0.085, 0.10, and 0.15 prepared by LRS and for $x = 0.085$ prepared by SSR. The activation energies for $x \leq 0.085$ are close to the reported values for the similar compositions.[10,21,24] For the samples prepared by LRS for different Co concentrations in Table 2, we can also see an obvious trend of the activation energy in a temperature range of 600 °C–800 °C: the apparent activation energy for the electrical conduction decreases continuously with Co content increasing up to 8.5 mol% and then drops abruptly when the Co content is further increased. The trend is consistent with the reported results of the activation energy of Co-doped LSGMs of other compositions.[9,10,21] The abrupt drop of the activation energy for the Co content larger than 8.5 mol% suggests that the hole conduction becomes dominant.[9,10] The high temperature activation energy (0.53 eV) for the sample of $x = 0.085$ prepared by LRS falls in a range of 0.51 eV–0.68 eV of the activation energy for ionic conductivity of Co-doped LSGM found by Khorkounov *et al.*,[32] suggesting the predominant ionic conductivity at higher temperatures. Nevertheless, the high temperature activation energies for the samples $x \geq 0.10$ prepared by LRS are much lower than the reported values for ionic conduction.

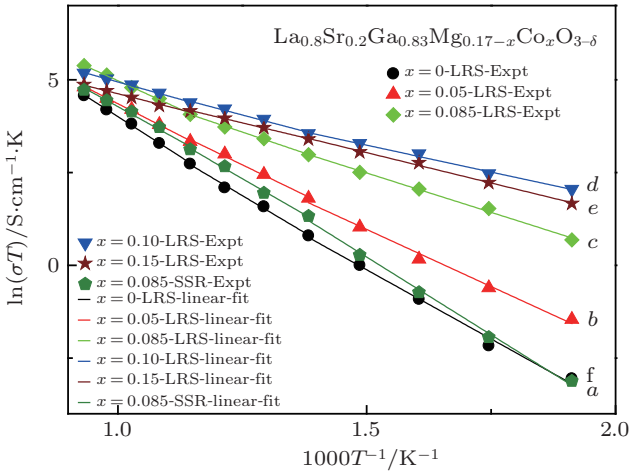


Fig. 10. (color online) Arrhenius plots of the total conductivities of $La_{0.8}Sr_{0.2}Ga_{0.83}Mg_{0.17-x}Co_xO_{3-\delta}$ with $x = 0.0$, 0.05, 0.085, 0.10, and 0.15, prepared by LRS with 1100-W laser power at 1 mm·s^{-1} scan speed and with $x = 0.085$, prepared by SSR (sintered at 1250 °C for 10 h, 1500 °C for 6 h, and 1600 °C for 2 h).

In order to confirm the conduction mechanisms of $La_{0.8}Sr_{0.2}Ga_{0.83}Mg_{0.17-x}Co_xO_{3-\delta}$ samples with different content values of Co doping, we measure the electrical conductivity as a function of the oxygen partial pressures ($p(O_2)$) of the samples at 800 °C as shown in Fig. 11. The electrical conductivity of the sample without Co doping ($x = 0$) prepared by LRS is nearly independent of the oxygen partial pressure in an oxygen partial pressure ($p(O_2)$) range from 10^{-19} atm to 0.98 atm, indicating an oxygen-ion conduction, which is in agreement with the reported results.[10,22] Figure 11 shows clearly that the samples with the Co content values $\leq$ 8.5 mol% prepared by LRS and SSR present ionic conductions in an oxygen partial pressure ($p(O_2)$) range from 10^{-16} atm to 0.98 atm and ionic mixed electronic conductions in an oxygen partial pressure ($p(O_2)$) range from 10^{-19} atm to 10^{-16} atm, whereas those with the Co content values $\geq$ 10.0 mol% present the characteristics of ionic mixed electronic conduction. Besides, the samples with the Co content values $\leq$ 8.5 mol% prepared by LRS have higher ionic conductivities than the sample without Co doping, which is in consistence with the results of Ishihara *et al.*[9,10] The improved oxide-ion conductivities of $La_{0.8}Sr_{0.2}Ga_{0.83}Mg_{0.17-x}Co_xO_{3-\delta}$ for $x \leq 0.085$ compared with the oxide-ion conductivity of the sample without Co doping may be brought about by the enhanced mobility of oxide ions by Co doping as revealed by previous study on the diffusion coefficients.[9] However, when Co content value is $\geq$ 10.0 mol%, the hole conduction may become more significant due to the formation of Co^{3+}, giving rise to free holes and resulting in an ionic mixed electronic conduction.

Figure 11 shows also that the ionic conductivity of $La_{0.8}Sr_{0.2}Ga_{0.83}Mg_{0.085}Co_{0.085}O_{3-\delta}$ prepared by LRS is much higher than by SSR. This demonstrates that in addition to the effect of Co doping, the unique microstructures of the samples generated during the laser rapid solidification process contribute also to the improved ionic conductivities. The relatively oriented growth of the spear-like or leaf-like grains with large and regular sizes and high relative densities greatly reduce the scattering probabilities of oxygen ions during migration.

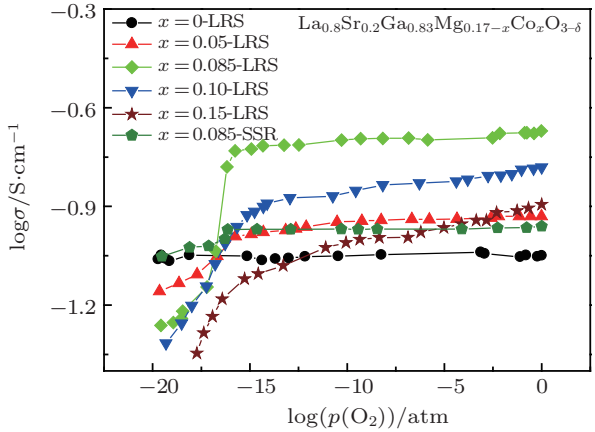


Fig. 11. (color online) The electrical conductivities measured each as a function of oxygen partial pressure at 800 °C for $La_{0.8}Sr_{0.2}Ga_{0.83}Mg_{0.17-x}Co_xO_{3-\delta}$ with $x = 0.0$, 0.05, 0.085, 0.10, and 0.15, synthesized by LRS with 1100-W laser power at 1 mm·s^{-1} scan speed and with $x = 0.085$, synthesized by SSR (sintered at 1250 °C for 10 h, 1500 °C for 6 h, and 1600 °C for 2 h).

Finally, we point out that the LRS is a unique technique for the syntheses of LSGM and Co-doped LSGM materials. With this technique, a sample with tens of grams can be produced in a few seconds. Besides the unique microstructures which cannot be obtained by conventional SSR methods, the samples prepared by LRS method also exhibit better electrical properties than by SSR methods. The disadvantages of LRS method are the requirements for a high power laser processing setup, precise control of the laser processing parameters such as laser power and scan speed to ensure fully reactions and avoid vaporization of the samples.

4. Conclusions

Laser rapid solidification (LRS) is used for synthesizing $La_{0.8}Sr_{0.2}Ga_{0.83}Mg_{0.17-x}Co_xO_{3-\delta}$ (LSGMs, x=0, 0.05, 0.085, 0.10, 0.15) materials. It is shown that the laser rapid solidification method is suitable for rapid sintering of the Co-doped LSGMs with controlled compositions. The samples prepared by LRS give rise to orderly arranged and densely packed unique spear-like or leaf-like microstructures and good electrical properties compared with by solid state reactions. It is shown that the samples with the Co content values $\leq$ 8.5 mol% exhibit ionic conductivities which increase with Co content increasing and are higher without Co doping in an oxygen partial pressure ($p(O_2)$) range from 10^{-16} atm to 0.98 atm at 800 °C. The ionic conductivity of $La_{0.8}Sr_{0.2}Ga_{0.83}Mg_{0.085}Co_{0.085}O_{3-\delta}$ prepared by LRS is much higher than by SSR. The improved ionic conductivities are attributed to the unique microstructures of the samples generated during laser rapid solidification. However, the samples with Co content values of $\geq$ 10.0 mol% present the characteristics of ionic mixed electronic conduction, which may result from the formation of Co^{3+} at higher doping levels.

References

[1] Fergus J W 2006 *J. Power Sources* **162** 30
[2] Haile S M 2003 *Acta Mater.* **51** 5981
[3] Xiang J, Guo Y T, Chu Y Q and Zhou G Z 2011 *Acta Phys. Sin.* **60** 027203 (in Chinese)
[4] Shen X Q, Wei T, Peng T G, Zhang Y, Lou K X and Xiang J 2009 *Acta Phys. Sin.* **58** 3402 (in Chinese)
[5] Wang X H and Xiang J 2008 *Acta Phys. Sin.* **57** 4417 (in Chinese)
[6] Zhang J, Liang E J, Sun Q and Jia Y 2012 *Chin. Phys. B* **21** 047201
[7] Ishihara T, Matsuda H and Takita Y 1994 *J. Am. Chem. Soc.* **116** 3801
[8] Huang K, Tichy R S and Goodenough J B 1998 *J. Am. Ceram. Soc.* **81** 2565
[9] Ishihara T, Akbay T, Furutani H and Takita Y 1998 *Solid State Ionics* **113–115** 585
[10] Ishihara T, Furutani H, Honda M, Yamada T, Shibayama T, Akbay T, Sakai N, Yokokawa H and Takita Y 1999 *Chem. Mater.* **11** 2081
[11] Trofimenko N and Ullmann H 1999 *Solid State Ionics* **118** 215
[12] Trofimenko N and Ullmann H 1999 *Solid State Ionics* **124** 263
[13] Stevenson J W, Hasinska K, Canfield N L and Armstrong T R 2000 *J. Electrochem. Soc.* **147** 3213
[14] Kharton V V, Viskup A P, Yaremchenko A A, Baker R T, Gharbage B, Mather G C, Figueiredo F M, Naumovich E N and Marques F M B 2000 *Solid State Ionics* **132** 119
[15] Yaremchenko A A, Shaula A L, Logvinovich D I, Kharton V V, Kovalevsky A V, Naumovich E N, Frade J R and Marques F M B 2003 *Mater. Chem. Phys.* **82** 684
[16] Ishihara T, Shibayama T, Nishiguchi H and Takita Y 2001 *J. Mater. Sci.* **36** 1125
[17] Enoki M, Yan J, Matsumoto H and Ishihara T 2006 *Solid State Ionics* **177** 2053
[18] Ishihara T, Tabuchi J, Ishikawa S, Yan J, Enoki M and Matsumoto H 2006 *Solid State Ionics* **177** 1949
[19] Gomes E, Marques F M B and Figueiredo F M 2008 *Solid State Ionics* **179** 1325
[20] Polini R, Falsetti A and Traversa E 2005 *J. Eur. Ceram. Soc.* **25** 2593
[21] Polini R, Falsetti A, Traversa E, Schäf O and Knauth P 2007 *J. Eur. Ceram. Soc.* **27** 4291
[22] Wang S Z, Wu L L and Liang Y 2007 *J. Power Sources* **166** 22
[23] Ishihara T, Ishikawa S, Yu C Y, Akbay T, Hosoi K, Nishiguchi H and Takita Y 2003 *Phys. Chem. Chem. Phys.* **5** 2257
[24] Xue J F, Shen Y, Zhou Q J, He T M and Han Y H 2010 *Int. J. Hydrogen Energy* **35** 294
[25] Zhang J, Liang E J and Zhang X H 2010 *J. Power Sources* **195** 6758
[26] Liang E J, Wu T A, Yuan B, Chao M J and Zhang W F 2007 *J. Phys D: Appl. Phys.* **40** 3219
[27] Liang E J, Wang J P, Xu E M, Du Z Y and Chao M J 2008 *J. Raman Spectrosc.* **39** 887
[28] Liang E J 2010 *Rec. Pat. Mater. Sci.* **3** 106
[29] Macdonald J R 1987 *Impedance Spectroscopy* (New York: Wiley) pp. 105–106
[30] Herle J V, McEvoy A J and Thampi K R 1994 *J. Mater. Sci.* **29** 3691
[31] Kosacki I, Anderson H U, Mizutani Y and Ukai K 2002 *Solid State Ionics* **152–153** 431
[32] Khorkounov B A, Näfe H and Aldinger F 2006 *J. Solid State Electrochem.* **10** 479